Quasiparticle density of states in layered superconductors under a magnetic field parallel to the *ab* plane: Determination of the gap structure of Sr_2RuO_4

Masafumi Udagawa, Youichi Yanase, and Masao Ogata
Department of Physics, University of Tokyo, Hongo, Tokyo 113-0033, Japan
(Received 17 December 2003; revised manuscript received 14 May 2004; published 17 November 2004)

We study the vortex state of a layered superconductor with vertical line nodes on its Fermi surface when a magnetic field is applied in the *ab*-plane direction. We rotate the magnetic field within the plane, and analyze the change of low-energy excitation spectrum. Our analysis is based on the microscopic Bogoliubov-de Gennes equation and a convenient approximate analytical method invented by Pesch and developed by Dahm *et al.* Both methods give consistent results. Near the upper critical field H_{c2}, we observe a larger zero-energy density of states (ZEDOS) when the magnetic field is applied in the nodal direction, while much below H_{c2}, larger ZEDOS is observed under a field in the anti-nodal direction. We give a natural interpretation to this crossover behavior in terms of contributions of quasiparticles propagating parallel and perpendicular to the applied field in the plane. We examine the recent field angle variation experiments of thermal conductivity and specific heat. Comparisons with our results suggest that special care should be taken to derive the position of line nodes from the experimental data. Combining the experimental data of the specific heat and our analyses, we conclude that Sr_2RuO_4 has a vertical-line-node-like structure in the direction of the *a* axis and the *b* axis.

DOI: 10.1103/PhysRevB.70.184515 PACS number(s): 74.25.Op, 74.25.Bt, 74.70.Pq

I. INTRODUCTION

Unconventional superconductors are among the most important materials in the modern condensed matter physics and may offer key insight into the effects of strong electron correlations. A number of superconductors—high-T_c cuprates, heavy-fermion metals, ruthenates, and organic compounds—exhibit unconventional behavior in the sense that the superconducting gap vanishes somewhere on the Fermi surface, resulting in power-law behaviors in various thermodynamic quantities. However, detailed gap structures are still controversial except for the cuprates. One of the difficulties in clarifying the gap structures will be the lack of experimental probes sensitive to quasiparticle momentum distribution.

Recently vortex states have been attracting much interest, because the positions of gap nodes can be determined from some physical quantities under a magnetic field applied parallel to the superconducting plane. For example, thermal conductivity[1–9] and specific heat[10–12] depend on the angle between the magnetic field and the superconducting gap nodes. Hence, by rotating the field within the plane and tracing the change of these quantities, one can obtain the information of the gap nodes. So far, a number of layered unconventional superconductors have been studied, including Sr_2RuO_4,[4,5,10] $CeCoIn_5$,[6,11] $\kappa-(ET)_2Cu(NCS)_2$,[7] YNi_2B_2C,[8,12] and $PrOs_4Sb_{12}$.[9]

However, it is found that some of these experiments show the behaviors incompatible with the results of theoretical analyses. For example, microscopic calculations show an existence of a vertical line-node-like structure in Sr_2RuO_4,[13–16] while a horizontal line node is persisted from the thermal conductivity experiments.[4,5] Probably these discrepancies are attributed to the lack of a firm theoretical basis in analyzing the experimental data.

Most studies on the vortex states have been limited to the case in which the magnetic field is applied perpendicular to the plane.[17–23] On the other hand, few microscopic analyses have been done in the case of a parallel magnetic field.[24,25]

In the analyses of the experimental data, a phenomenological Doppler-shift method has often been used to derive the position of the gap nodes. According to this method, larger density of states (DOS) is obtained when the field is applied in the antinodal direction than in the nodal direction.[26,27] However, it has been pointed out that the Doppler-shift method is quite unreliable in some cases.[28] This method is based on the approximation that low-energy excitations in a vortex state consist solely of Doppler-shifted nodal quasiparticles. It can be justified only at low magnetic fields. The effect of core states neglected in this formalism becomes important at high magnetic fields and may alter the field-orientational dependence of DOS. Therefore, it is crucial to establish a microscopic theory in the case of a parallel magnetic field, and to give a correct interpretation of experiments.

In this paper, we present a detailed study of quasiparticle DOS in a layered superconductor under a magnetic field applied parallel to the *ab* plane. We will focus on Sr_2RuO_4, in which positions of the line nodes are still controversial.[4,5,10,14–16,24,29] A cylindrical Fermi surface with vertical line nodes of *f*-wave symmetry is assumed. We concentrate on the two cases where a magnetic field is in the nodal direction, and in the antinodal direction. Using the obtained low-energy quasiparticle states, we interpret the experimental data. It turns out that specific heat measurement is superior to thermal conductivity as a probe to detect the position of gap nodes, since DOS does not suffer from the large two-fold component with respect to the magnetic field.[24] Our analysis is based on the microscopic Bogoliubov-de Gennes equation and an approximate analytical method invented by Pesch[30] and recently developed by Dahm, Graser, Iniotakis, and Schopohl.[28]

In the next section, the calculational formulation is described. In Sec. III, we will show our results and discussion on the experiments. Section IV is devoted to a conclusion.

II. FORMULATION

A. Model and some features

First, we introduce some general features of our model. We study a quasi-two-dimensional layered superconductor which has a cylindrical Fermi surface with small *c*-axis dispersion. Thus we assume a dispersion relation,

$$\epsilon_{\mathbf{p}} = \frac{\mathbf{p_{ab}}^2}{2m_{ab}} - v_c \cos k_z, \tag{1}$$

where $\mathbf{p_{ab}}$ is the momentum in the *ab* plane and the *c*-axis wave number k_z varies in the interval $[-\pi, \pi]$. In this system, the Fermi velocity can be written in the following form:

$$\mathbf{v}_F = v_F(\cos\phi \mathbf{e}_a + \sin\phi \mathbf{e}_b + \epsilon \sin k_z \mathbf{e}_c), \tag{2}$$

with $v_F = P_F/m_{ab}$, and $v_c = \epsilon v_F$. Here, the azimuthal angle ϕ varies between 0 and 2π. The *c*-axis dispersion exists due to a small inter-layer hopping.

In this paper, we consider a spin-triplet superconductivity with its **d** vector parallel to the *c* axis, i.e., the order parameter is

$$\hat{\Delta}(\mathbf{k}) = \begin{pmatrix} 0 & \Delta(\mathbf{k}) \\ \Delta(\mathbf{k}) & 0 \end{pmatrix}. \tag{3}$$

The momentum dependence of $\Delta(\mathbf{k})$ is assumed to be

$$\Delta(\mathbf{k}) = \Delta_0(\hat{k}_a + i\hat{k}_b)(\hat{k}_a^2 - \hat{k}_b^2). \tag{4}$$

This is the simplest model of the chiral state with four-fold symmetric vertical line nodes at $|\hat{k}_a| = |\hat{k}_b|$ whose effect is the main subject in this paper. Note that exact positions of nodes are not important in the following discussion. The qualitative behavior of low-energy DOS is determined by the angle between an applied field and line nodes.

In order to study the vortex lattice state under a magnetic field parallel to the *ab* plane, we assume a spatial variation of the order parameter, $\psi(\mathbf{r})\Delta(\mathbf{k})$. Here $\psi(\mathbf{r})$ represents the Abrikosov vortex square lattice obtained by solving linearized Ginzburg-Landau (GL) equation at $H = H_{c2}$.[31] The isotropic GL equation at $H = H_{c2}$ is given by

$$\xi^2\left[\frac{\partial^2}{\partial r_\perp^2} + \left(\frac{\partial}{\partial z} - i\frac{r_\perp}{\xi^2}\right)^2\right]\psi_I(\mathbf{r}) + \psi_I(\mathbf{r}) = 0, \tag{5}$$

where ξ is the coherence length and $r_\perp$ denotes the coordinate for the axis in the *ab* plane perpendicular to the magnetic field. Here, we adopt a Landau gauge,

$$\mathbf{A}(\mathbf{r}) = H r_\perp \mathbf{e}_c. \tag{6}$$

From Eq. (5), one can obtain the isotropic Abrikosov vortex square lattice,

$$\psi_I(\mathbf{r}) = 2^{1/4}\sum_{n=-\infty}^{\infty} \exp\left(i2\pi n\frac{z}{L} - \pi\left(\frac{r_\perp}{L} - n\right)^2\right). \tag{7}$$

Here a new parameter L satisfies the following condition:

$$L^2 = 2\pi\xi^2 = \frac{\phi_0}{H_{c2}}, \tag{8}$$

and represents the spatial period.

Since Sr_2RuO_4 has a strong anisotropy between the *ab* plane and the *c* axis, we have to take account of this anisotropy. For the anisotropic superconductors with coherence lengths ξ_{ab} in the *ab* plane and ξ_c along the *c* axis, the GL equation at $H = H_{c2}$ reads as

$$\left[\xi_{ab}^2\frac{\partial^2}{\partial r_\perp^2} + \xi_c^2\left(\frac{\partial}{\partial z} - i\frac{r_\perp}{\xi_{ab}\xi_c}\right)^2\right]\psi(\mathbf{r}) + \psi(\mathbf{r}) = 0. \tag{9}$$

Equation (9) is obtained from Eq. (5) by transforming $r_\perp \to (\xi/\xi_{ab})r_\perp$ and $z \to (\xi/\xi_c)z$. Then, the anisotropic Abrikosov lattice $\psi(\mathbf{r})$ can be obtained from the same transformation of $r_\perp$ and z in Eq. (7), which gives

$$\psi(\mathbf{r}) = 2^{1/4}\sum_{n=-\infty}^{\infty} \exp\left(i2\pi n\frac{z}{L_c} - \pi\left(\frac{r_\perp}{L_{ab}} - n\right)^2\right). \tag{10}$$

Here, $L_c = (\xi_c/\xi)L$ and $L_{ab} = (\xi_{ab}/\xi)L$. In the following calculation, we put $\xi_c = \epsilon\xi_{ab}$, hence $L_c = \epsilon L_{ab}$. Note that $\psi(\mathbf{r})$ is equal to zero at the positions $r_\perp = L_{ab}\left(m + \frac{1}{2}\right)$ and $z = L_c\left(l + \frac{1}{2}\right)$ with arbitrary integers m and l, representing the centers of vortices.

Since $\psi(\mathbf{r})$ represents an Abrikosov square vortex lattice at $H = H_{c2}$, we have to assume a vortex lattice structure for $0 < H < H_{c2}$. We assume the following periodicity of the vortex lattice:

$$Ł_j(H) = \sqrt{2\pi}\xi_j\sqrt{\frac{H_{c2}}{H}} \quad (j = c, ab), \tag{11}$$

because the size of a vortex unit cell is inversely proportional to H. Note that we have assumed that H is uniformly applied to the system because Ginzburg-Landau parameter κ of Sr_2RuO_4 is much larger than 1.

B. Numerical solution of the Bogoliubov-de Gennes equation

Using the above dispersion relations and spatially inhomogeneous superconducting order parameter, $\hat{\Delta}(\mathbf{k})\psi(\mathbf{r})$, we solve the Bogoliubov-de Gennes (BdG) equation, which is considered to be the most reliable approach:[31]

$$\begin{pmatrix} \hat{H}_0 & \hat{\Delta}(-i\nabla)\psi\left(\frac{\mathbf{r}+\mathbf{r}'}{2}\right) \\ -\hat{\Delta}^*(i\nabla)\psi^*\left(\frac{\mathbf{r}+\mathbf{r}'}{2}\right) & -\hat{H}_0^* \end{pmatrix} \times \begin{pmatrix} u(\mathbf{r}) \\ v(\mathbf{r}) \end{pmatrix}\Bigg|_{\mathbf{r}'\to\mathbf{r}} = E\begin{pmatrix} u(\mathbf{r}) \\ v(\mathbf{r}) \end{pmatrix}, \tag{12}$$

where

$$\hat{H}_0 = \begin{pmatrix} \frac{1}{2m_{ab}}\left(\mathbf{P}_{ab} - \frac{e}{c}\mathbf{A}\right)^2 - \mu & 0 \\ 0 & \frac{1}{2m_{ab}}\left(\mathbf{P}_{ab} - \frac{e}{c}\mathbf{A}\right)^2 - \mu \end{pmatrix} \tag{13}$$

and

$$u(\mathbf{r}) = \begin{pmatrix} u_\uparrow(\mathbf{r}) \\ u_\downarrow(\mathbf{r}) \end{pmatrix}, \quad v(\mathbf{r}) = \begin{pmatrix} v_\uparrow(\mathbf{r}) \\ v_\downarrow(\mathbf{r}) \end{pmatrix}. \tag{14}$$

Here we assumed $\epsilon \ll 1$, and neglected the effect of the c-axis dispersion. This prescription corresponds to neglecting a coherence along the c-axis direction, or in the quasiclassical sense, to taking account of only the trajectories parallel to the ab plane. We will discuss the details of this prescription later in the next section. Equation (12) can be decoupled into a 2×2 matrix equation for $(u_\uparrow, v_\downarrow)$ and $(u_\downarrow, v_\uparrow)$. Since both the pairs satisfy the same equation, we can work on only one of them, say, $(u_\uparrow, v_\downarrow)$.

We numerically diagonalize Eq. (12) by discretizing the coordinate $\mathbf{r}$, and obtain sets of eigenvalues E_K and eigenfunctions $\mathbf{(}u_K(\mathbf{r}), v_K(\mathbf{r})\mathbf{)}$. Using the obtained eigenfunctions, we calculate the DOS:

$$\nu_{BdG}(\epsilon) = \sum_{E_K>0} \int d\mathbf{r}[|u_K(\mathbf{r})|^2 \delta(\epsilon - E_K) + |v_K(\mathbf{r})|^2 \delta(\epsilon + E_K)]. \tag{15}$$

Due to the translational symmetry along the magnetic field, the momentum parallel to the vortices, $p_\parallel$, becomes a good quantum number. On the other hand, since momentum normal to the magnetic field, $p_\perp$, is not a conserved quantity, $p_\perp$ has a finite width $\delta p_\perp$ for each eigenstate. Nevertheless, $\delta p_\perp / p_\perp$ is much smaller than 1 (of the order of $1/k_F\xi_{ab}$), not too much below T_c. Thus we can use an approximation, $p_\perp = \sqrt{p_F^2 - p_\parallel^2}$. In the quasiclassical meaning, we consider that a quasiparticle represented by $\mathbf{(}u_K(\mathbf{r}), v_K(\mathbf{r})\mathbf{)}$ has a trajectory with momentum $(\sqrt{p_F^2 - p_\parallel^2}, p_\parallel)$. Therefore we define

$$\theta = \arctan\left(\frac{\sqrt{p_F^2 - p_\parallel^2}}{p_\parallel}\right) \quad (0 \leqslant \theta \leqslant \pi), \tag{16}$$

for each eigenfunction, which represents an angle between the magnetic field and quasiparticle trajectory. Using this θ, we decompose the zero-energy DOS into contributions from quasiparticles propagating in the θ direction. In the following we call this an angle-resolved zero-energy DOS.

C. Approximate analytical approach using a method by Pesch and Dahm *et al.*

As a complementary method, we also study the problem using an approximate analytical method invented by Pesch[30] and developed by Dahm *et al.*[28,32] In this paper, we call this the PD method. We will compare the obtained results in both methods. Near H_{c2}, spatial variation of the order parameter is small. Hence, in the Eilenberger equations, it is allowed to replace the normal component of quasiclassical Green's functions, g, by its spatial average over a vortex unit cell. With this averaged quasiclassical Green's function, we can calculate various observable quantities (e.g. DOS) in the averaged form over a vortex unit cell. According to Dahm *et al.*,[28] this approximation gives the result quantitatively in agreement with that obtained in the rigorous Eilenberger equation, even much below H_{c2}.

Here, we summarize the main results of this method. For details, see Ref. 28. We assume that a spatial variation of the order parameter is described by $\psi(\mathbf{r})$, or the Abrikosov vortex lattice introduced in Sec. II A. Then, the averaged density of states $\nu_{PD}(\epsilon)$ (in the unit of DOS for the normal state ν_0) can be written in the following form:

$$\nu_{PD}(\epsilon) = \left\langle \mathrm{Re}\frac{1}{\sqrt{1 + P(\mathbf{v_F}, i\omega_n \to \epsilon + i0)}} \right\rangle_F, \tag{17}$$

where $\langle \cdots \rangle_F$ means an average over the Fermi surface, and in our model, $P(\mathbf{v_F}, i\omega_n)$ is written as

$$P(\mathbf{v_F}, i\omega_n) = \frac{4|\Delta(\mathbf{k})|^2}{\pi |\mathbf{v}_{\mathbf{F}\perp}|^2}\left[1 - \frac{\sqrt{2}\omega_n}{|\mathbf{v}_{\mathbf{F}\perp}|} e^{2{\omega_n}^2/\pi|\mathbf{v}_{\mathbf{F}\perp}|^2} \times \mathrm{erfc}\left(\frac{\sqrt{2}\omega_n}{\sqrt{\pi}|\mathbf{v}_{\mathbf{F}\perp}|}\right)\right], \tag{18}$$

where $\mathbf{v}_{\mathbf{F}\perp}$ is the projection of the scaled Fermi velocity onto the plane normal to the magnetic field,

$$\mathbf{v}_{\mathbf{F}\perp} = v_F\left(\frac{\cos\theta}{L_{ab}}\mathbf{e}_{ab} + \frac{\epsilon \sin k_z}{L_c}\mathbf{e}_c\right). \tag{19}$$

Since $\nu_{PD}(\epsilon)$ in Eq. (17) is written as an average over the Fermi surface, we can decompose $\nu_{PD}(\epsilon)$ into the contributions from the quasiparticles with $\mathbf{v}_F$. Defining θ as an angle between $\mathbf{v}_F$ and the magnetic field, we can obtain an angle-resolved zero-energy DOS, $\nu_{PD}(0,\theta)$, as

$$\nu_{PD}(0,\theta) = \mathrm{Re}\frac{1}{\sqrt{1 + P(\mathbf{v_F}(\theta), i\omega_n \to +i0)}}. \tag{20}$$

Before showing our results, let us compare the above two methods. When we solve BdG equation, we take account of the spatial variation of g. However the three-dimensional calculation is very difficult practically, so that we have neglected the coherence along the c axis. Whereas in the approximate analytical method introduced in this subsection, the coherence along the c axis is taken into account. However the spatial variation of g is neglected. In this sense, the two methods are complementary with each other.

III. RESULTS

In this chapter, we will show the results obtained in the two methods introduced in the previous chapter. We study mainly two cases in which a magnetic field is applied in the nodal direction and in the antinodal direction. DOS is considered to take its minimum and maximum in one and the other of these two cases, respectively. This quantity can be observed experimentally. We will also show the angle-

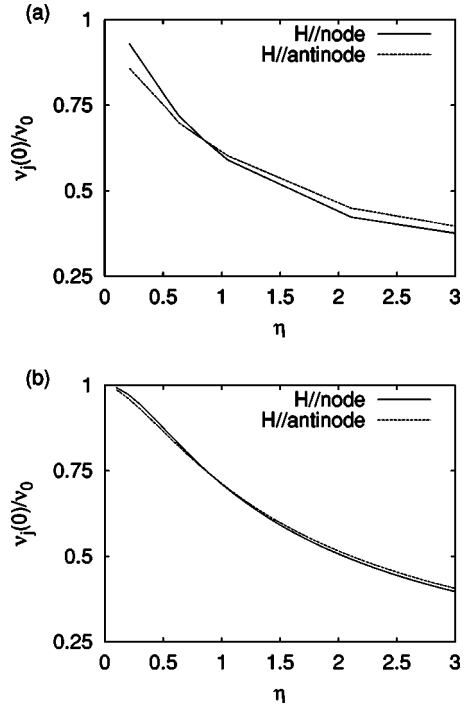

FIG. 1. The η dependence of the zero-energy density of states calculated with (a) the BdG method and (b) the PD method. The solid line shows ZEDOS for the $\mathbf{H}\|$node, i.e. $\nu_n(0)/\nu_0$, while the dashed line shows ZEDOS for the $\mathbf{H}\|$antinode, i.e. $\nu_a(0)/\nu_0$. ZEDOS is normalized to the normal-state value.

resolved zero-energy DOS, $\nu(0,\theta)$, introduced in the previous section. Note that θ is an angle between the applied magnetic field and the quasiparticle trajectory.

As regards the magnetic field dependences, we notice that our results are approximately determined by a single parameter, namely the reduced order parameter $\eta(H)$ defined by

$$\eta(H) = \sqrt{\frac{2}{\pi}}\frac{\Delta_0(H)Ł_{ab}(H)}{v_F}. \tag{21}$$

Thus, without knowing the precise H dependence of Δ_0, we can study general H dependences of our results. [$\eta(H)$ corresponds to $z(\epsilon_n/\Delta)^{-1}$ in Ref. 28.] Note that $\eta(H)$ monotonically decreases as an increasing magnetic field H and becomes 0 when H reaches H_{c2}.

A. Zero-energy density of states (ZEDOS)

First, we will discuss the density of states right at zero energy. In Fig. 1, we show our results of the η dependence of ZEDOS, calculated with the BdG and the PD methods. ZEDOS under a field in the nodal direction is denoted as $\nu_n(0)$ and in the anti-nodal direction as $\nu_a(0)$. Both $\nu_n(0)$ and $\nu_a(0)$ are normalized to the normal-state value ν_0. We can see that the two methods give qualitatively the same results. Figure 1 shows that in a high magnetic field or when H is close to H_{c2} (low η), $\nu_n(0) > \nu_a(0)$, while in a low magnetic field (high η), $\nu_a(0) > \nu_n(0)$.

In order to understand this crossover behavior, we study the angle-resolved ZEDOS obtained with the BdG method

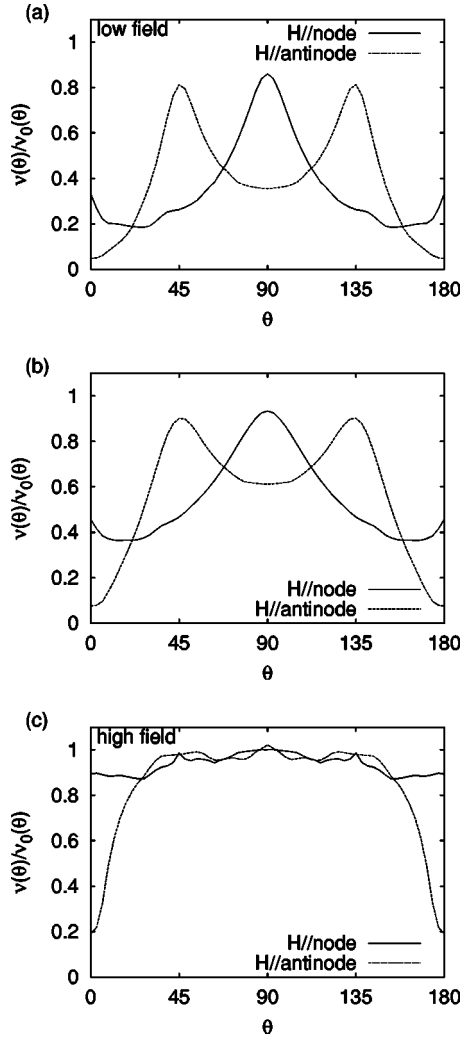

FIG. 2. Angle-resolved ZEDOS $\nu(0,\theta)$ calculated by the BdG method. They are normalized by a value without $\mathbf{H}$. θ is measured from the field direction. (a) $\eta=2.11$, (b) $\eta=1.05$, and (c) $\eta=0.21$.

for several values of η (Fig. 2). In a low field case [Fig. 2(a)], we can see that narrow regions on the Fermi surface are mainly contributing to the total ZEDOS. In the case of the $\mathbf{H}\|$node, a sharp peak appears at $\theta=90°$ which corresponds to the nodal direction perpendicular to the magnetic field. In contrast, the nodal quasiparticles running parallel to the field ($\theta=0°, 180°$) give a much smaller contribution to ZEDOS. In the case of the $\mathbf{H}\|$antinode, we can observe two peaks of the same height at $\theta=45°$ and 135°, which correspond to the nodal directions.

With an increasing magnetic field (decreasing η) [Fig. 2(b)], the nodal peaks become broader and there appears a contribution which does not have a strong θ dependence. The latter can be considered as the contribution from the core states. This is because the decrease of the order parameter amplitude makes it easier for low-energy quasiparticles to propagate independent of the direction of $\mathbf{H}$. As for the quasi-particles running parallel to the field (i.e. $\theta=0°, 180°$), we can see a big difference between the two cases. In the case of the $\mathbf{H}\|$node, the contribution from the field direction becomes larger with increasing field strength, while in the

case of the **H**∥antinode, the contribution from this direction remains small.

When the field strength is increased (η is decreased) further [Fig. 2(c)], nodal peaks become too broad to be identified. In most of the Fermi surface, the angle-resolved ZEDOS recover the normal-state value. Nevertheless, an appreciable difference still exists for the quasiparticles running parallel to the field.

We can understand the nature of this difference by using the idea of quasi-classical trajectories of quasiparticles.[33–35] There are two ways in which quasiparticles contribute to ZEDOS. One is the Doppler shift by the supercurrent:[17] If a quasiparticle runs in the nodal direction and not parallel to the field, it can contribute to ZEDOS because of the Doppler shift. This contribution appears as the peaks in Fig. 2. The other is the formation of Andreev bound states: Roughly speaking, if the order parameter changes its sign on a trajectory of a quasiparticle, Andreev bound states are formed. This gives a finite contribution to ZEDOS.

Now let us consider the quasiparticles running approximately parallel to the field. The density of states is zero right along the magnetic field, whether the field is in the nodal or antinodal direction. However, differences arise when the quasiparticles propagate along a direction slightly off the field. In the case of the **H**∥antinode, little density of states appear since the Doppler shift is weak and the phase of the order parameter changes very slowly. Hence, quasiparticles are hampered by finite and nearly uniform order parameter and cannot contribute to ZEDOS, no matter how small (high) the order parameter amplitude (magnetic field) is. In contrast, in the case of the **H**∥node, order parameter is so small that the slight Doppler shift or sign change of the order parameter can lead to small but finite ZEDOS. This is why the angle-resolved ZEDOS at $\theta=0°$ is suppressed in the case of the **H**∥antinode in a high magnetic field region. Note that the quasiparticles running right through a vortex core feel no superconducting gap. However, contributions from such quasiparticles are considerably small.

The idea we have noted here has some similarities with that given in Ref. 24. In Ref. 24, it was pointed out that thermal conductivity takes a maximum value when heat current is perpendicular to the magnetic field, since the largest contribution to ZEDOS comes from quasiparticles running perpendicular to the field.

Next, let us compare the above results with those obtained in the PD method. In Fig. 3, we show the angle-resolved ZEDOS, Eq. (20), after integrating over k_z. In most parts of the Fermi surface, we observe much the same behavior as the BdG results. However, as for the quasiparticles running in the field direction ($\theta=0°, 180°$), the PD method gives a larger angle-resolved ZEDOS than that in BdG method. We attribute this difference to the prescription we made in solving the BdG equations, that is, a neglect of the *c*-axis dispersion term. This prescription corresponds to considering only the quasiparticles running parallel to the *ab* plane, i.e., limiting the *c*-axis component of the Fermi velocity k_z to 0. Hence, our prescription in the BdG method enhances the contribution of the quasiparticles with $k_z=0$. In order to confirm this, we plot the angle-resolved ZEDOS obtained from Eq. (20) with $k_z=0$ in Fig. 4. Comparing it with Fig. 2(a), a

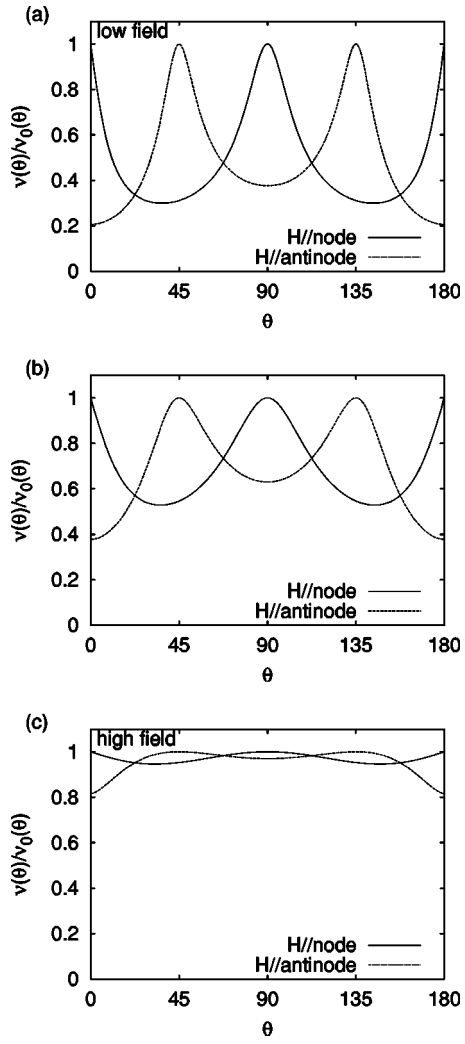

FIG. 3. Angle-resolved ZEDOS, $\nu(0,\theta)$, calculated in the PD method. θ is measured from the field direction. (a) $\eta=2.11$, (b) $\eta=1.05$, and (c) $\eta=0.21$.

quantitative agreement can be seen in $\theta\sim 0°$ and 180°. Since the quasiparticles with $k_z=0$ and $\theta=0°$ are perfectly parallel to **H**, they give a little contribution to ZEDOS.

The above difference in angle-resolved ZEDOS at $\theta=0°$ and 180° in the two methods leads to the difference in the total ZEDOS shown in Fig. 1 for the high magnetic field case ($\eta\sim 0.1$). Since this difference comes mainly from the con-

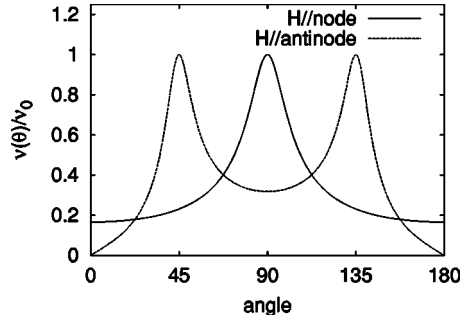

FIG. 4. Angle-resolved ZEDOS calculated with the PD method with $k_z=0$ for $\eta=2.11$.

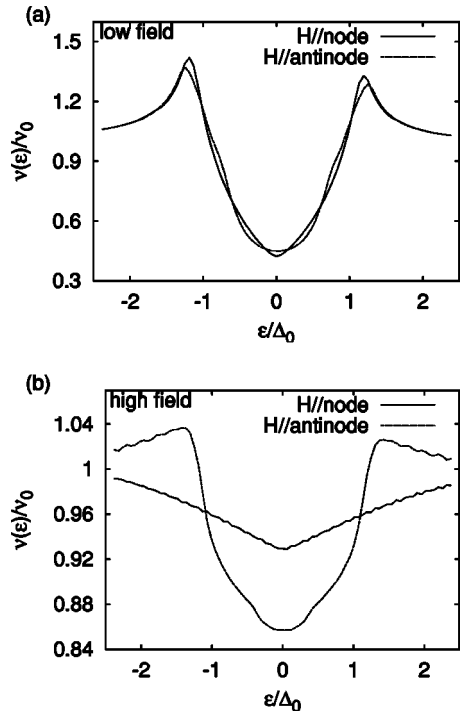

FIG. 5. Finite-energy DOS (normalized to the normal-state value) calculated with the BdG method. (a) $\eta=2.11$ and (b) $\eta=0.21$.

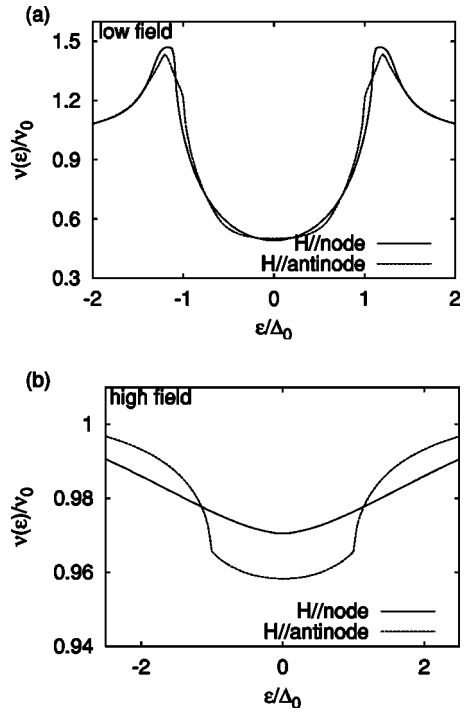

FIG. 6. Finite-energy DOS (normalized to the normal-state value) calculated in the PD method. (a) $\eta=2.11$ and (b) $\eta=0.21$.

tribution at $\theta\sim 0°$, the BdG analysis overestimates the difference in ZEDOS.

Here we briefly summarize the main results in this subsection. In a low magnetic field region, ZEDOS is dominated by nodal quasiparticles which have a finite momentum normal to the field. In this region, we have $\nu_a(0)>\nu_n(0)$, since in the case of the $\mathbf{H}\|$node, two out of the four nodes are parallel to the field, thus unable to contribute to ZEDOS, while in the case of the $\mathbf{H}\|$antinode, all the four nodes contribute to ZEDOS. In a high magnetic field region, on the other hand, the difference between $\nu_a(0)$ and $\nu_n(0)$ comes from the behavior of quasiparticles running in the field direction ($\theta\sim 0°$). In the case of the $\mathbf{H}\|$antinode, those quasiparticles are hampered by finite and uniform order parameter and cannot contribute to ZEDOS, while in the case of the $\mathbf{H}\|$node, they can. Therefore, we have $\nu_n(0)>\nu_a(0)$ in this field region.

B. Density of states at finite energy

Next, we will show our results for DOS at finite energy. This is particularly important when we discuss the experimental data, which depend on the density of states at $0\lesssim\epsilon\lesssim k_BT$. In Figs. 5 and 6, we show DOS obtained with the BdG and the PD methods, respectively.

Let us first discuss the high magnetic field region [Figs. 5(b) and 6(b)], we observe a sharp rise in DOS at $|\epsilon|\sim\Delta_0$ reminiscent of a coherence peak in the case of the $\mathbf{H}\|$antinode, while it is absent in the case of the $\mathbf{H}\|$node. This character of DOS reflects the behavior of the quasiparticles running parallel to the field. Since they feel a finite order parameter in the case of the $\mathbf{H}\|$antinode, they tend to form a coherence peak. This coherence-peak-like structure appears more clearly in the BdG result due to our prescription as discussed in the previous subsection.

In this high magnetic field region, we observe $\nu_n(\epsilon)>\nu_a(\epsilon)$ for $0\lesssim|\epsilon|\lesssim\Delta_0$ independent of the calculational methods. Therefore, if the thermal conductivity or the specific heat is measured in this field region with a rotating magnetic field, maximum will be observed when the field is applied in the nodal direction.

Results in a low magnetic field region are shown in Figs. 5(a) and 6(a). In this field region, as we have discussed in the previous subsection, $\nu_a(0)>\nu_n(0)$ at zero energy. However, as shown in Fig. 5(a) and 6(a), $\nu_a(\epsilon)$ and $\nu_n(\epsilon)$ cross at $|\epsilon|\sim 0.2\Delta_0$. For $|\epsilon|>0.2\Delta_0$ we have an opposite inequality $\nu_n(\epsilon)>\nu_a(\epsilon)$. This means that when we take experimental data at a temperature $T\gtrsim 0.2\Delta_0$ with a rotating magnetic field within the plane, we will observe very small angle variation, because the effects of lower-energy DOS and higher-energy DOS cancel each other.

C. Interpretations of the experimental data

In this subsection, we discuss how to interpret the experimental data of the thermal conductivity and the specific heat, in connection with our analyses.

The thermal conductivity[4,5] and the specific heat[10] of Sr_2RuO_4 have been measured under a rotating in-plane field by several groups. In the experiments of magnetothermal conductivity,[4,5] they found no angle variation except in the vicinity of H_{c2}. They attributed the angle variation near H_{c2} to the anisotropy of H_{c2} itself, and denied the existence of

vertical line nodes in Sr_2RuO_4. On the other hand, in the experiment of specific heat,[10] a fourfold oscillation is found at a lower field, in addition to the angle variation near H_{c2}. The specific heat shows a maximum at $\mathbf{H}\|[110]$ in low fields, while its maximum is observed at $\mathbf{H}\|[100]$ near H_{c2}. These two measurements seem to provide incompatible results. However, our theoretical analysis gives an answer to this contradiction in the following way.

First we discuss why the thermal conductivity does not show the fourfold oscillation in the low field region. As we show in the previous subsection, a reversal of $\nu_n(\epsilon)$ and $\nu_a(\epsilon)$ occurs in the low field region at $\epsilon \sim 0.2\Delta_0$. In order to observe the anisotropy of ZEDOS, a contribution from the higher energy part of DOS must be removed. However, the thermal conductivity has been measured at rather high temperatures $T=0.2-0.3T_c$, where the effect of the high energy part of DOS mixes inevitably as we note in the previous subsection. Hence, it is no wonder that the anisotropy of ZEDOS cannot be observed. On the other hand, the measurement of specific heat was conducted at lower temperatures $T<0.1T_c$. Therefore the specific heat is sensitive to ZEDOS. Furthermore, note that the specific heat is more sensitive to the low energy part of DOS than the thermal conductivity. These will be the reason why only the specific heat shows the fourfold oscillation.

Combining the above considerations, we determine the position of line nodes. In the measurement of the specific heat, the maximum was found at $\mathbf{H}\|[110]$, while we have $\nu_a(0) > \nu_n(0)$ in a low magnetic field region. Therefore, we conclude that the line nodes exist in the direction $[\pm 100]$ and $[0 \pm 10]$.

In Secs. III A and III B, we have shown that $\nu_n(\epsilon) > \nu_a(\epsilon)$ for $0 \lesssim |\epsilon| \lesssim \Delta_0$ in a high magnetic field region. Therefore, in this field region, there is a possibility that we can observe a fourfold oscillation both in the thermal conductivity and the specific heat, aside from the effect of the anisotropy in H_{c2}.

In summary, we can explain the data of specific heat and thermal conductivity simultaneously by assuming the vertical lines nodes along the $[\pm 100]$ axis. A line-node-like structure in this direction is expected in the γ band from the relation between the Fermi surface and crystal symmetry,[14] and has been confirmed in the microscopic analysis.[15] Strictly speaking, these are not line nodes, because the excitation gap is small but finite. However, tiny gaps behave like line nodes at finite temperatures.

IV. CONCLUSIONS

We studied the density of states in the vortex state of a layered superconductor with vertical line nodes on the cylindrical Fermi surface under a field parallel to the *ab* plane. We investigated the angle variation of DOS with the changing field strength. The Bogoliubov-de Gennes equation and an approximate analytical method by Pesch and Dahm *et al.* were solved. We found that a field in the nodal direction gives larger zero-energy density of states in a higher magnetic field region, whereas a field in the anti-nodal direction results in larger zero-energy density of states in a lower magnetic field region. This crossover phenomenon is naturally understood in terms of the angle-resolved ZEDOS. In a higher field region, under a field applied in the anti-nodal direction, quasiparticles running parallel to the field is hampered by a spatially uniform order parameter, and thus gives a smaller contribution to ZEDOS compared with the case of the $\mathbf{H}\|$ node. In a lower field region, nodal quasiparticles not parallel to the field contribute significantly to ZEDOS. Therefore, when the field is applied in the anti-nodal direction, four such nodes are available, which leads to the larger ZEDOS compared with the case of the $\mathbf{H}\|$ node, where only two such nodes are available.

We investigated the angle variation of the density of states at finite energy. We found that in a low magnetic field region, DOS at $\epsilon \gtrsim 0.2\Delta_0$ shows a maximum when the field is parallel to the node, while ZEDOS shows a minimum for this field direction. On the basis of this fine structure of DOS, we discussed why the thermal conductivity does not show fourfold oscillation in the low field region. Finally, combining the experimental data of the specific heat and our analyses, we conclude that Sr_2RuO_4 has vertical line-node-like structure in the direction of the *a* axis and the *b* axis.

We note that both in BdG and PD analyses, we have assumed Abrikosov vortex function $\Psi(\mathbf{r})$ as a spatial variation of order parameter. Some of our results may be quantitatively altered by mixing of higher Landau levels. However, we believe that our conclusions do not change qualitatively.[36]

We are grateful to K. Deguchi for teaching us his experimental results. We also thank N. Yoshida for helpful discussions.

[1] F. Yu, M. B. Salamon, A. J. Leggett, W. C. Lee, and D. M. Ginsberg, Phys. Rev. Lett. **74**, 5136 (1995).
[2] H. Aubin, K. Behnia, M. Ribault, R. Gagnon, and L. Taillefer, Phys. Rev. Lett. **78**, 2624 (1997).
[3] R. Ocaña and P. Esquinazi, Phys. Rev. Lett. **87**, 167006 (2001).
[4] K. Izawa, H. Takahashi, H. Yamaguchi, Yuji Matsuda, M. Suzuki, T. Sasaki, T. Fukase, Y. Yoshida, R. Settai, and Y. Onuki, Phys. Rev. Lett. **86**, 2653 (2001).
[5] M. A. Tanatar, M. Suzuki, S. Nagai, Z. Q. Mao, Y. Maeno, and T. Ishiguro, Phys. Rev. Lett. **86**, 2649 (2001).
[6] K. Izawa, H. Yamaguchi, Yuji Matsuda, H. Shishido, R. Settai, and Y. Onuki, Phys. Rev. Lett. **87**, 057002 (2001).
[7] K. Izawa, H. Yamaguchi, T. Sasaki, and Y. Matsuda, Phys. Rev. Lett. **88**, 027002 (2002).
[8] K. Izawa, K. Kamata, Y. Nakajima, Y. Matsuda, T. Watanabe, M. Nohara, H. Takagi, P. Thalmeier, and K. Maki, Phys. Rev. Lett. **89**, 137006 (2002).
[9] K. Izawa, Y. Nakajima, J. Goryo, Y. Matsuda, S. Osaki, H. Sugawara, H. Sato, P. Thalmeier, and K. Maki, Phys. Rev. Lett. **90**, 117001 (2003).

[10] K. Deguchi, Z. Q. Mao, H. Yaguchi, and Y. Maeno, Phys. Rev. Lett. **92**, 047002 (2004).
[11] H. Aoki, T. Sakakibara, H. Shishido, R. Settai, Y. Onuki, P. Miranović, and K. Machida, cond-mat/0312012.
[12] T. Park, M. B. Salamon, E. M. Choi, H. J. Kim, and S-I. Lee, Phys. Rev. Lett. **90**, 177001 (2003).
[13] K. Kuroki, M. Ogata, R. Arita, and H. Aoki, Phys. Rev. B **63**, 060506(R) (2001).
[14] K. Miyake and O. Narikiyo, Phys. Rev. Lett. **83**, 1423 (1999).
[15] T. Nomura and K. Yamada, J. Phys. Soc. Jpn. **71**, 404 (2002).
[16] M. J. Graf and A. V. Balatsky, Phys. Rev. B **62**, 9697 (2002).
[17] G. E. Volovik, JETP Lett. **58**, 469 (1993).
[18] N. Schopohl and K. Maki, Phys. Rev. B **52**, 490 (1995).
[19] Y. Wang and A. H. MacDonald, Phys. Rev. B **52**, R3876 (1995).
[20] M. Ichioka, N. Hayashi, N. Enomoto, and K. Machida, Phys. Rev. B **53**, 15 316 (1996).
[21] A. Himeda, M. Ogata, Y. Tanaka, and S. Kashiwaya, J. Phys. Soc. Jpn. **66**, 3367 (1997).
[22] D. Knapp, C. Kallin, and A. J. Berlinsky, Phys. Rev. B **64**, 014502 (2001).
[23] H. Tsuchiura, M. Ogata, Y. Tanaka, and S. Kashiwaya, Phys. Rev. B **68**, 012509 (2003).
[24] L. Tewordt and D. Fay, Phys. Rev. B **64**, 024528 (2001).
[25] P. Miranović, N. Nakai, M. Ichioka, and K. Machida, Phys. Rev. B **68**, 052501 (2003).
[26] I. Vekhter, P. J. Hirschfeld, J. P. Carbotte, and E. J. Nicol, Phys. Rev. B **59**, R9023 (1999).
[27] H. Won and K. Maki, Europhys. Lett. **54**, 248 (2001).
[28] T. Dahm, S. Graser, C. Iniotakis, and N. Schopohl, Phys. Rev. B **66**, 144515 (2002).
[29] Y. Tanaka, K. Kuroki, Y. Tanuma, and S. Kashiwaya, J. Phys. Soc. Jpn. **72**, 2157 (2003).
[30] W. Pesch, Z. Phys. B: Condens. Matter **21**, 263 (1975); P. Klimesch and W. Pesch, J. Low Temp. Phys. **32**, 869 (1978).
[31] See, for example, P. G. de Gennes, *Superconductivity of Metals and Alloys* (Perseus Books, 1999).
[32] S. Graser, T. Dahm, and N. Schopohl, Phys. Rev. B **69**, 014511 (2004).
[33] J. W. Serene and D. Rainer, Phys. Rep. **101**, 221 (1983).
[34] N. Kopnin, *Theory of Nonequilibrium Superconductivity* (Oxford University Press, Oxford, 2001).
[35] N. Schopohl, cond-mat/9804064.
[36] M. Takigawa, M. Ichioka, and K. Machida, Eur. Phys. J. B **27**, 303 (2002).